Revista Brasileira de Ciências Ambientais
Brazilian Journal of Environmental Sciences

Wavelet transform for medium-range streamflows projections in national interconnected system

Transformada em ondeletas para projeções de vazões em médio prazo no sistema nacional interconectado

Carlos Eduardo Sousa Lima[1], *Marx Vinicius Maciel da Silva*[1], *Cleiton da Silva Silveira*[1], *Francisco das Chagas Vasconcelos Junior*[2]

ABSTRACT

This study aimed to analyze the variability of average annual streamflow time series of the National Interconnected System (NIS) (Brazil) and create a projection model of future streamflow scenarios from 3 to 10 years using wavelet transform (WT). The streamflow time series were used and divided into two periods, namely, 1931–2005 and 2006–2017, for calibration and verification, respectively. The annual series was standardized, and by the WT, it was decomposed into two bands plus the residue for each base posts (BP) for later reconstruction. Then, an autoregressive (AR) model per band and residue was made. The projection was obtained by adding the AR models. For performance evaluation, a qualitative analysis of the cumulative probability distribution of the projected years and an analysis of the likelihood were performed. The model identified the probability distribution function of the projected years and obtained a likelihood ratio of > 1 in most SIN regions, indicating that this methodology can capture the medium-range variability.

Keywords: autoregressive wavelets; National Interconnected System; climate variability; streamflow projection.

RESUMO

O presente trabalho objetiva analisar a variabilidade das séries temporais de vazão média anual do Sistema Nacional Interconectado (SIN) (Brasil) e criar um modelo de projeção de cenários de vazão de três até dez anos utilizando transformada em ondeleta. As séries temporais de vazão foram divididas em dois períodos — 1931 até 2005 e 2006 até 2017 — para calibração e validação, respectivamente. As séries anuais foram padronizadas e, por meio da transformada em ondeleta, foram decompostas em duas bandas e no resíduo para cada Posto Base (BP) para uma futura reconstrução. Em seguida foi feito um modelo autorregressivo por banda e para o resíduo. A projeção foi obtida pelo somatório das projeções desses modelos autorregressivos. Para avaliar a *performance*, uma análise qualitativa da distribuição de probabilidade acumulada dos anos projetados foi realizada e a verossimilhança foi calculada. O modelo identificou a distribuição de probabilidade dos anos projetados e obteve verossimilhança maior que 1 na maioria das regiões do SIN, o que indica que essa metodologia é capaz de capturar a variabilidade de médio prazo.

Palavras-chave: ondeletas autoregressivas; Sistema Nacional Interconectado; variabilidade climática; projeção de vazão.

[1]Universidade Federal do Ceará – Fortaleza (CE), Brazil.

[2]Fundação Cearense de Meteorologia e Recursos Hídricos – Fortaleza (CE), Brazil.

Correspondence address: Carlos Eduardo Sousa Lima – Departamento de Engenharia Hidráulica e Ambiental – Campus Pici, Bloco 713 – Pici – CEP: 60455-900 – Fortaleza (CE), Brazil. E-mail: eduardolima@alu.ufc.br

Conflicts of interest: The authors declared that there is no conflict of interest.

Funding: Fundação Cearense de Apoio ao Desenvolvimento Científico e Tecnológico (FUNCAP) and Conselho Nacional de Desenvolvimento Científico e Tecnológico – Brazil (Previsões mensais de vazões para o Sistema Interligado Nacional [SIN] utilizando multimodelos, no. 409724/2018-1).

Received on: 02/09/2021. Accepted on: 10/24/2021.

https://doi.org/10.5327/Z2217694781048

Introduction

The expansion planning of the Brazilian electric system is composed, among other activities, of computational simulations of future electric energy system configurations (Costa et al., 2007). In these simulations, it is sought to locate and measure future electricity and energy needs, as well as adjusting entry schedules of generation projects, among others. Such adjustments are made following criteria that mainly aim at the security of supply and minimization of investment and operating costs.

To supply the growing power demand, the country has strongly invested in their power energy generation, mainly in hydroelectric plants over whole country. In Brazil, power generation went from 223 billion kilowatts hours in 1990 to 626 billion in 2019, with an average rate growth of approximately 3.5% per year. The hydropower participation was always prominent in its power plant grid, varying from 93 to 64% in the same period (IEA, 2020). The hydroelectric generation and planning of the hydropower sector in Brazil presents correlation with the water stocks in the hydroelectric power plants reservoirs and their inflows.

Emergency thermoelectric plants are used to supply the country's power demand, mostly in critical dry periods, with low volume in reservoirs. These thermoelectric plants are considered virtual reservoirs because they provide security of supply when the water reservoirs are low and relief the needs of stocking water to deals with inflow uncertainty. The hydropower plants are operated in combination with thermoelectric plants by the National System Operator (ONS in Portuguese) and the junction of all sources that comprises the Brazilian power grid called National Interconnected System (NIS).

The variation of the river flow is influenced by several factors, among which the precipitation in the contribution basin and land use changes are highlighted. Therefore, the hegemony of hydroelectricity in the Brazilian electric energy matrix imposes cautious analysis on river regimes and their temporal variation patterns, considering the significant impact that these variations can produce in the energy supply and consequently throughout the national economy (Alves et al., 2013).

Power systems, such as the Brazilian one, are subject to impacts arising from climate variability and change and shifts in power production and consumption. Thus, climate variability can condition the risk associated with the generation of electric energy. The possibility of quantification of risks allows decisions to be taken so that the impacts of adverse events are minimized, thus reducing the degree of vulnerability of a given region.

A large part of the interannual climate variability over South America is modulated by the atmospheric patterns in response to the El Niño-Southern Oscillation (ENSO) phenomenon in the equatorial Pacific (Grimm et al., 2020) and by the meridional gradient of sea surface temperature (SST) anomalies over the tropical Atlantic (Kayano et al., 2018). The combination of the anomalous atmospheric circulations induced by the spatial patterns of SSTs on the equatorial Pacific and tropical Atlantic Oceans affects the latitudinal position of the Intertropical Convergence Zone (ITCZ) over the Atlantic in addition to the moisture transport into the continent, influencing the seasonal precipitation anomalies over the northern and central portions of South America.

Kayano et al. (2018) reported the fluctuations of SST anomalies in the Northern Tropical Atlantic and the Southern Tropical Atlantic as part of two decadal modes of distinct periodicities separated by the ITCZ. Zhang et al. (1997) described another characteristic Pacific Ocean SST oscillation, in addition to ENSO, occurring on an interdecadal scale. This phenomenon has been called the Pacific Decadal Oscillation (PDO).

The PDO has two phases: in the negative phase, the characteristics are negative anomalies of SST in the tropical Pacific and, simultaneously, positive SST anomalies in the extratropical Pacific, with tendency for the occurrence of a larger number of La Niña episodes, which are also likely to be more intense. Conversely, in the positive phase of PDO, the tendency is for a larger number of El Niño episodes that tend to be more intense. In contrast, there is a lower number of La Niña, which tends to be less expressive. PDO fluctuations have two main periodicities, one presenting a cycle of 15–25 years and the other presenting a cycle of 50–70 years (Kayano et al., 2019; Wang et al., 2019).

The influences of this interdecadal scale oscillation on South American climate variability were also investigated by Grimm and Saboia (2015) and references therein. These studies have demonstrated that the PDO phenomenon influences the volume of precipitation. Furthermore, extreme rainfall events are more likely to occur when both ENSO and PDO are in the same phase.

Grimm et al. (2020) and references quoted therein pointed to the influence of ENSO and Atlantic Multidecadal Oscillation (AMO) on precipitation over South America, in the respective interannual and interdecadal oscillation scale. Rocha and Souza Filho (2020) have identified a strong coherence between the changes of ONS streamflow time series and SST interdecadal oscillation patterns (AMO and PDO) in the key stations of ONS, including Sobradinho, Itaipú, and Furnas.

Considering the importance of hydroelectric generation for the Brazilian NIS and the various mechanisms responsible for the climate variability in this region, which associate a risk to this system, this study aimed to propose a model for the medium-term projection for the NIS, based on the climatic variability of the series of naturalized streamflow of the ONS using the wavelet transform (WT) method. This study is organized as follows: an overview of the NIS structure and describes the methods and data, the results, and, finally, discussion and conclusion.

Methodology

The methodology utilized covers climate variability and trend analysis to identify patterns through the streamflow data. WT and band decomposition are performed to bring up the prominent modes of variation. Then, statistical modeling takes place, building, validating, and applying the autoregressive wavelets (WAR) model to produce streamflow medium-range forecasts. A workflow scheme is depicted in Figure 1.

National Interconnected System

NIS is responsible for the production and transmission of electric energy in Brazil. NIS is a large hydrothermal system with predominance of hydroelectric plants. Only 1.7% of the country's electricity production capacity is outside the NIS, in small isolated systems located mainly in the Amazon region (ONS, 2016).

For forecasting outflows, ONS generally adopts a subset of basins, called base post (BP). In the rest of the places of use, the flows are predicted through monthly linear regressions based on the data provided in the BP to complement the forecasts of flow for the whole NIS. ONS currently works with 88 BPs that are representative of the various regional hydrologic regimes found in Brazil (ONS, 2010b). These BPs are listed in Figure 2 and are used in the flow projections of this study. Moreover, four reference BPs were adopted for a more extensive analysis due their relevance, including Tucuruí, Sobradinho, Itaipú, and Água Vermelha. These reference BPs are highlighted in Figure 2.

Data, trend, and variability analysis

To calibrate and evaluate the dexterity of the model, the ONS naturalized flow database was used for the period from 1931 to 2016 for the SIN. The series of annual average naturalized flows were divided into two periods, namely, 1931–2005 and 2006–2017, for calibration and verification, respectively. Projections are also made for the period from 2017 to 2026.

Knowing that the observed flow is composed of both natural processes and anthropogenic activities, the naturalized streamflow, generally speaking, is an estimate of the natural flow obtained by removal of anthropogenic impacts on the observed streamflow. These impacts are generated by human activities, such as reservoir operations upstream of the streamflow gauge, water withdrawal, and river flow alteration by control infrastructures, among others. More information can be accessed in ONS (2010) and Terrier et al. (2021).

Regarding the approach, the methodologies of trend/variability evaluation can be distributed in two groups: classical methods and modern methods. The classical methods used in this study were 10-year moving average and Mann–Kendall–Sen (MKS) for annual mean flow.

The MKS method is composed of nonparametric Mann–Kendall test and nonparametric Sen's slope estimate procedure. These methods are used, respectively, for trend detection and, if there is, trend magnitude determination. The MKS is widely used in trend analysis because it does not require initial assumption about the probability distribution and has a low sensitivity to outliers. More information can be obtained from a study by Moreira and Naghettini (2016).

Among the modern methods, the WT analysis (Torrence and Compo, 1998) of the standardized annual series was considered. This analysis consists of the decomposition of the series into bands, as described, for all the stations of SIN and the discussion of the band relationship with temporal series variability.

The WAR model

The WAR model contains at least six steps:

- Standardization of the annual series based on its mean and standard deviation (Equation 1).

$$z_i = x - \frac{x}{\sigma_x} \quad (1)$$

Where:

x: the data to be standardized;

$\bar{x}$: the mean of the series;

σ_x: the standard deviation of the series.

- Analysis of the WT power spectrum for the identification of the most energetic bands, filtration of the series for the bands of greater energy, and reconstruction of filtered series in time domain for each considered band;

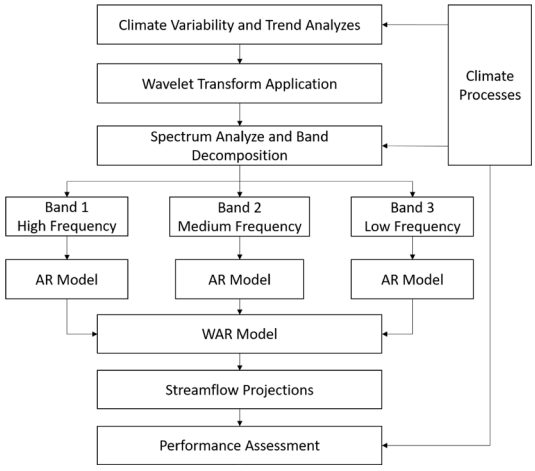

Figure 1 – Workflow diagram of the methodology used in this study.
AR: autoregressive; WAR: autoregressive wavelets.

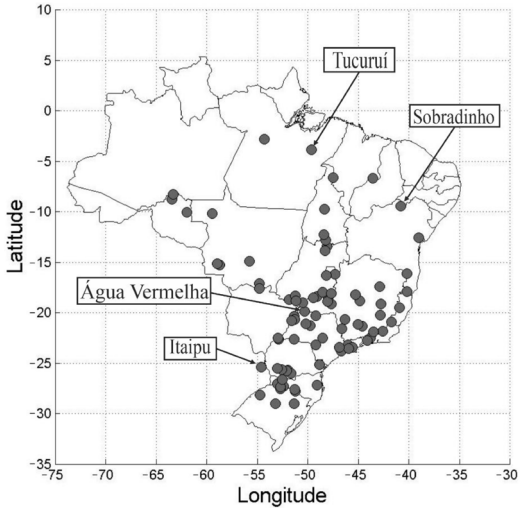

Figure 2 – Eighty-eight base gauge stations highlighting the four reference base posts adopted in this study.

- Obtaining the parameters of the autoregressive (AR) models that are generated for each one of reconstructed series in time domain of each adopted band. This procedure is repeated for all BPs;
- Noise generation for each AR model obtained from the mean and standard deviation of the difference between the bands and the value obtained by the AR model in the calibration period;
- Integration of the bands, considering that they are orthogonal, then the sum of projected bands is equal to projected streamflow.

Wavelet transform

One of the methods used in this study to characterize the variability both in space and in time is the WT (Torrence and Compo, 1998; Morettin, 1999). This method is widely utilized for the determination of the dominant variability modes and the variation of these modes throughout a nonstationary time series, enabling the decomposition of this kind of time series in a time–frequency domain.

The wavelet transform is defined in terms of a convolution integral between the analyzed signal and a known wavelet function. The Morlet wavelet continuous function was considered for this analysis and is given by Equation 2:

$$\psi(\eta) = \pi^{-1/4} e^{i\omega_0 \eta} e^{-\eta^2/2} \quad (2)$$

with w_0=6 and η=t/s

where:
t: time;
s: the scale of the wavelet;
w_0: the nondimensional frequency representing a wave modulated by a Gaussian envelope.

This function is complex and has characteristics similar to those of the analyzed time series, such as symmetry or asymmetry, and sudden or soft temporal variation. The algorithm used was developed by Torrence and Compo (1998). More details about WT can be found at Morettin (1999).

In this study, the WT was performed to decompose the streamflow time series in specific frequency bands. Beside this, the signal of each adopted frequency band in the decomposition was reconstructed in time domain, being used as input to the AR model.

Decomposition and reconstruction of the bands

The signal power of the global spectrum of the wavelet can be used to identify the most significant variation frequencies of a time series. The power is associated with the signal strength of the historical series for a given frequency or band (range) of frequencies (Torrence and Compo, 1998).

To create the WAR model, an important step is the decomposition of the bands, which consists of analyzing the global energy spectrum over the time series and then identifying the frequencies, or frequency bands, of greater power and filter the series for these bands. The signal decomposition is done to obtain the wavelet coefficients in the transformed domain (frequency domain).

As suggested by Alves et al. (2013), three bands were used in this study: a high frequency, 1–8 years; a medium frequency, 9–39 years; and a low frequency, > 40 years (residue).

After the signal decomposition in both high- and medium-frequency bands, the signals of these bands were reconstructed in time domain. For low-frequency band, considering that the wavelets and their bands are orthogonal functions, so the correlation between them is not significant, then the reconstructed low-frequency band in time domain can be obtained using the Equation 3:

$$R(i) = Q(i) - Q_1(i) - Q_2(i) \quad (3)$$

Where:
$Q(i)$: the annual mean streamflow value;
$Q_1(i)$: the value of the reconstructed high-frequency band (1–8 years) at i year;
$Q_2(i)$: the value of the reconstructed medium-frequency band (9–39 years) at i year;
$R(i)$: the value of the reconstructed low-frequency band (> 40 years).

Autoregressive model

After the signal reconstruction, an AR model is applied to each band, considering that they are orthogonal, given by Equation 4:

$$z_i^p = \sum_{i=1}^{b} \left(ARs_b(i) + ARs_{R(i)}(i) \right) \quad (4)$$

Where:
ARs_b: the autoregressive model of each band;
ARs_R: the autoregressive model of the residue.

A linear regression of the data is then performed, considering the previous years as predictors. The linear regression is given by Equation 5:

$$z_i^p = \varepsilon_1 + \sum_{j=i-n}^{i-1} z_j . \beta_n \quad (5)$$

Where:
z_j: the years considered as predictors;
βn: the coefficient calculated for each predictor;
ε_1: the bias/noise/residue;
n: the number of terms used in the AR model;
z_i^p: the set of values projected by the model for the period of p years.

The period used for the calibration of the parameters was from 1931 to 2006 in SIN, all with lag1 (1 year). The determination of ε_1

is done by generating m values randomly distributed in a normal multivariate function of mean, standard deviation, and covariance of the difference between the estimated and observed variables with lag1 over the course of 1931–2006. Thus, z_i^1 has m possible scenarios. The generation of the forecast with lag2 admits that all the scenarios generated for z_i^1 are plausible futures, with the previous years being predictors of the projected year. It stands out that m is an arbitrary value; in this study, it was adopted that m is equal to 1,000.

By definition, the original time series can be considered equal to the sum of the adopted frequencies bands reconstructed in time domain. Thus, the projected streamflow is equal the sum of the projected adopted bands, which were already been reconstructed in time domain before the application of AR model.

Model performance evaluation

After calculating streamflow projections for the region of interest, it is necessary to evaluate the performance of the proposed models. For the statistical models based on wavelet series, the qualitative analysis of the cumulative probability distribution of the projected years' period and an analysis of the likelihood between observation and projection are performed. It is worth noting that the purpose of the WAR model is to identify the probability distribution of the set of projected years and not specifically a 1-year forecast.

Maximum likelihood estimator

To calculate this estimator, it is necessary to define the likelihood function. The principle of likelihood states that "a statistical inference must be consistent with the hypothesis that the best explanation of a data set is provided by $\hat{\theta}$, a value of θ which maximizes the likelihood function." Intuitively, maximizing likelihood means getting the population most likely to have generated the sample.

In case of the regression model, the parameter vector of interest is given as Equation 6:

$$\theta' = (\beta', \sigma^2) \tag{6}$$

and defining L as a function of β' and σ^2 (Equation 7):

$$L(\beta, \sigma^2) = \prod_{i=1}^{n} f_{Y_i}(y_i|\beta, \sigma^2) \tag{7}$$

Finding the vector of estimated parameters that maximize the likelihood function is equivalent to maximizing likelihood. Therefore, to obtain this vector, the likelihood is derived in relation to each parameter and equals zero. This is the usual calculation method. For this, the median of the set of scenarios generated per year is approximated to a gamma distribution function and compared to the gamma distribution of the climatology.

The calculation of the projection performance, using the projection of the WAR and the climatology, in comparison to the total observed data, is attained using Equation 8:

$$\text{Performance} = \left(\frac{L(\beta,\sigma^2)_{\text{projection}}}{L(\beta,\sigma^2)_{\text{climatology}}}\right)^{\frac{1}{n}} \tag{8}$$

Where:
n: the number of years of the historical series utilized here.

When Performance > 1, it means that there was an improve on the forecast in relation to the climatology. Instead, when Performance > 1, it means that there was a worsening in projection.

Results and Discussion

Variability analysis

Streamflow time series can present several variability modes in different timescales, which can be conditioned by simultaneous action of many atmospheric systems of various temporal scales and the dynamic of their interactions. Due to these multi-scale meteorological phenomena, their combination determines the weather state in a given temporal scale and, consequently, the variability of the hydrologic cycle components. Furthermore, climate changes and alterations in the land use of a basin can modify the runoff patterns and create trends in the temporal series.

The annual series of average flow of SIN stations present different traces of trends (Mann–Kendall method and Sen's declivity) in Brazil. Figure 3 indicates that, as for the trend signal, there are three areas in different situations in the country: positive tendency (south regions: Mato Grosso do Sul and São Paulo), negative (northeast regions: Espírito Santo and Minas Gerais), and the absence of trend (further regions and states).

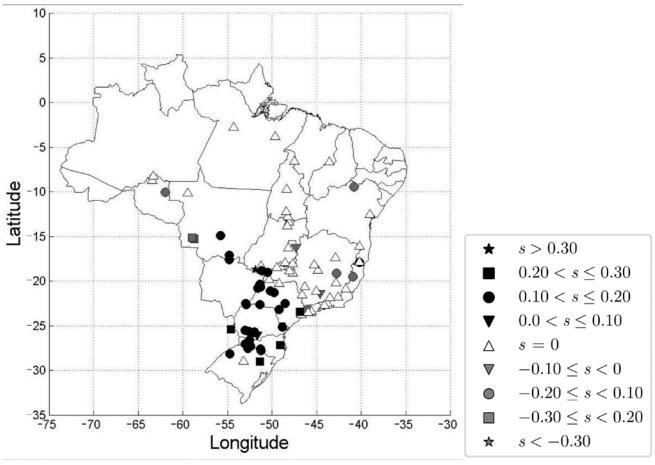

Figure 3 – Slope of the trend line of the Mann–Kendall–Sen test (s) for the variable z (standardized annual flow, according to Equation 1) for the period from 1931 to 2016.

The naturalized flows of Sobradinho, Água Vermelha, Tucuruí, and Itaipú in the period from 1931 to 2016 illustrate the variation modes in different temporal scales. There is an interannual variation of the average annual flow in these stations; for example, Sobradinho in the Northeast subsystem of the SIN has years with average values between 2,000 and 4,000 m^3/s, that is, there is a multiplicative factor greater than 2 between the minimum and the maximum, as can be seen in Figure 4. A similar behavior can be seen in other SIN subsystems; for example, in Tucuruí at the north of the country, the flow rate ranges from 6,000 and 14,000 m^3/s, and in Água Vermelha at the Southeast/Midwest subsystem, the flow rate ranges from 1,200 to 2,500 m^3/s. In Itaipú, despite presenting a trace of positive trend in the average annual flow, there is a sign of interannual variability, with flow rates in the period from 1931 to 1950 ranging between 6,000 and 10,000 m^3/s, as shown in Figure 4 where the interannual variability is explained between 30 and 45% of the variance of the historical series.

Besides the significant interannual variability, a series of annual average flow indicates significant hydrologic decadal variability, especially in the series of North, Northeast, and Southeast of SIN, for example, in a period of 10 years the average value is 3,000 m^3/s in the operation of Sobradinho, while in the other period of 10 years the average value decreases to approximately 2,500 m^3/s (Figure 4A). This behavior is also evidenced in the exploitation of Tucuruí, with a period of 10 years where the average value is 12,000 m^3/s and the other with the average value of approximately 9,000 m^3/s (Figure 4B).

This evidences a possible low-frequency variation mode, because this behavior is recurring along the whole time series. This variability can introduce in the water systems the alternation of consecutive wet and dry years. In the case of consecutive dry years, it should intensify the water rationing policies and the reduction in the granting of water use permission.

The lower frequency variability modes shape the climate on a global scale (Wang et al., 2012). These variability modes occur in the Pacific and Atlantic Oceans, overlapped and influenced by interannual modes, such as ENSO, and, as already mentioned, can influence the effects of these variabilities on South America. Rocha and Souza Filho (2020) detected low-frequency anomalies in the SST of Pacific (PDO) and Atlantic (AMO) in the period 1931–2016 with change-point analysis. The cold (C) and warm (W) phases of PDO and AMO detected were in the following periods: W-AMO (1931–1963 and 1995–2016), W-PDO (1931–1943, 1976–1998, and 2014–2016), C-AMO (1964–1994), and C-PDO (1944-1975 and 1999–2013). These periods are very close to the phases of PDO and AMO reported by Kayano et al. (2019) and, respectively, by Mantua et al. (1997) and Zhang and Delworth (2006).

The temporal series of Sobradinho in the period from 1932 to 1942 shows some years with average annual value lower than the historic mean, coincident with periods of the warm phase of PDO and AMO. In the next period, between 1943 and 1950, the annual flow in this exploitation reached higher values which are twice the historical mean, period that comprises the end of the warm phase and beginning of the cold phase of PDO, and according to Zhang and Delworth (2006), also within the minimum point of the warm phase of AMO.

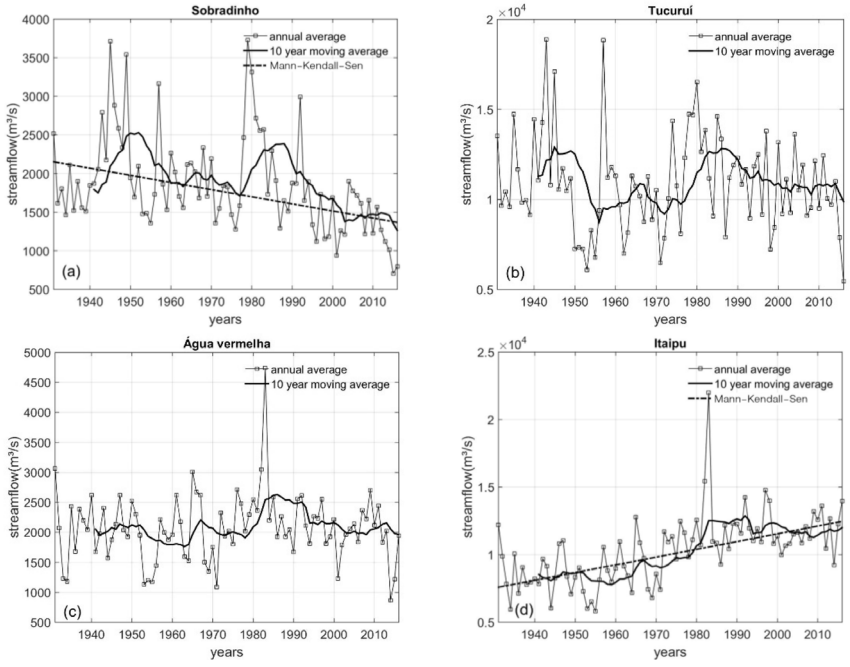

Figure 4 – Time series of annual average flow of some hydroelectric exploitations in the SIN: (A) Sobradinho; (B) Tucuruí; (C) Água Vermelha; (D) Itaipú.

In the period from 1973 to 1980, the AMO reached minimum points in the cold phase, coincident with maximum flow, according to the historical series. The period from 1963 to 1970 is a transition period between phases of AMO and a weak cold phase of the PDO, which is consistent with annual flow close to the historical mean. According to Rocha and Souza Filho (2020), the period between 2014 and 2016 was a warm phase of both PDO and AMO. In this period, the annual average streamflow of Sobradinho reached to the minimum of the entire series.

Especially on the Northeast region of Brazil (NEB), the principal phenomenon responsible for the rainfalls is the ITCZ, which migrates from the north to the south along the year. Naturally when closer to the coastal area of NEB, it causes higher precipitations, and consequently, flows there. Therefore, when AMO is in the cold phase, there is a tendency that the water of the North Atlantic is cooler than that in the South Atlantic, which indicates a higher possibility of precipitation in the region, and the reciprocal is also accepted.

The flow response of Tucuruí (Figure 4B) resembles to that of Sobradinho (Figure 4A); however, the impact of the warm and cold phases of the phenomena seems more intense in this region. In the Southern and Southeastern regions of the country, the Pacific affects the flow in an opposite way; therefore, the Água Vermelha (Figure 4C) flow series in the period from 1977 to 1995, in the warm phase of PDO, presented the annual value of around 20% higher than the annual mean of the period between 1931 and 2016.

Itaipú shows a clearly defined positive trend (Figure 4D); however, the flow fluctuations are lower in the warm phase of AMO and higher in the cold phase. Different mechanisms can act as modulators in the large-scale pattern in the ocean–atmosphere interaction, changing the basic state of southern circulation over South America and the South Atlantic Ocean and leading to variation in the precipitation pattern in the Southeastern and Southern Brazil in this timescale. Further analysis is required to understand the cause and effect of these variations.

Figure 5 shows the spatial distribution of the variation's proportions explained by high-, mean, and low-frequency bands, respectively. The high-frequency band (Figure 5A) is responsible for more than 45% of the variance in most of the series of annual average flow of SIN, indicating strong dependency of the interannual variability.

In the Midwest and Northeast regions, the high-frequency bands is responsible for at least 45% of the variance in most of the stations, similar to the stations localized in the extreme north of the country and in the coastal part of Southeast region. This behavior indicates that the signal associated with the interannual and decadal variability prevails over the tendency and the medium- and low-frequency variation modes.

Figure 5B shows that the mean frequency band is responsible for more values between 15% and 30% of the variance in the flow series of the stations at Southern region and east of the Southeast region, in the state of São Paulo. In the Midwest region and part of Northeast, in the northern part of the North and in the coast of the Southeast, the mean band frequency is responsible for more than 30% of the series variance.

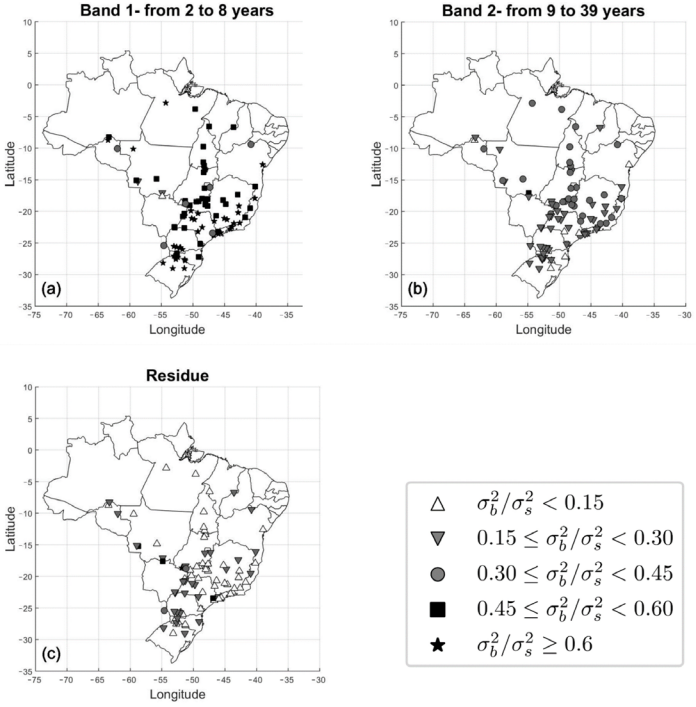

Figure 5 – Percentage of the explained variance for each band variation. (A) 2–8 years band, (B) 9–39 years band, and (C) residual band. σ_b^2 is the variance of the reconstructed series by the specific band and σ_s^2 is the variance of the original time series.

Figure 5C shows that in most part of the country, the low-frequency band is responsible for at least 15% of the variance in the flow series, except in some stations in the South, Midwest, and Southeast of the country, where it has a pronounced positive trend, according to Figure 3.

WAR model analysis

Figure 6 shows the WAR model calibration for different bands for Água Vermelha, Sobradinho, and Itaipú. The model represents well the low- and mean frequency bands, with bias close to zero in these bands. However, for the high-frequency band, the model softens the majority of the minimums and maximums, indicating high uncertainty and randomness in this band. There is a periodic oscillation in the low-frequency band, associated with a periodic oscillation in the mean frequency band with period between 10 and 20 years. The model captures well the low-frequency band, mainly in Itaipú and Água Vermelha, where there is a coincident phase inversion with the AMO phase.

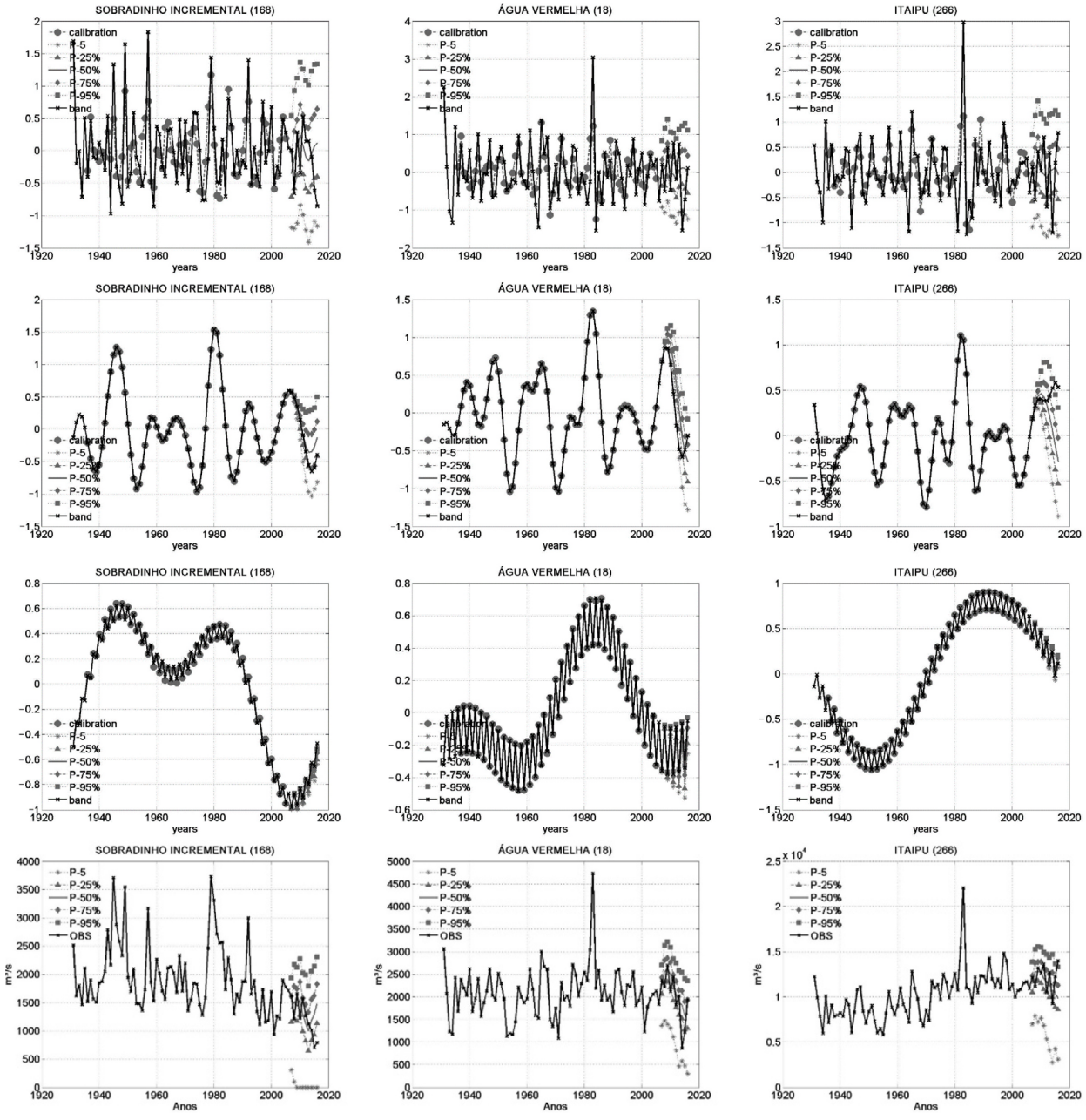

Figure 6 – Frequency bands of the wavelet transform, calibration, and projection of the WAR model. From top to bottom and left to right: 2–8 years band, 9–39 years band, and residue for Sobradinho, Água Vermelha e Itaipú.

The main flow peaks in Sobradinho are followed by maximum in the mean frequency band; as shown in the previous section, they are associated with the onset of the cold phase in the PDO.

The negative trend in Sobradinho (Figure 4A) is represented in the low-frequency band, especially since the 1990s when this band reaches values well below those obtained in others periods of the century. In the 1940s and beginning of the 1980s, the mean frequency band reaches maximum peaks (2,500 m^3/s), a value 25% above the time series average.

In the Água Vermelha station, the low-frequency band presented phase change in the second half of the 20th century, with strong peak in the 1980s. The influence of this band on the historical series and its inversion may have led to a period of lower flow for the next 30 years, especially between 2003 and 2016 when the mean and low-frequency band reached minimum point. In the 1950s, when the mean and low-frequency bands presented minimum values, the annual mean flow for consecutive years was lower than 1,500 m^3/s, at least 30% below the historical average value between 1931 and 2016. In the period of 1968–1971, the temporal series also reached values lower than 1,500 m^3/s coinciding with a minimum point of the mean frequency band, indicating that this phase may influence the flow distributions. Moreover, in the 1980s, there was a coincidence between the maximum of the three bands, which led to anomalous years above average.

In Itaipú, the positive trend (Figure 4D) is well characterized by the low-frequency band, especially since the 1980s when this band reached positive values, with maximum point in the 1990s. The possible phase inversion of this band may indicate reduction in the flow of this sector.

As for the projections to the period of 2007–2016, the noise amplitude grows with the horizon of the projection, which seems consistent with the uncertainty representation associated with climatic processes. The high-frequency band shows noise with high amplitude, higher than one standard deviation for Água Vermelha, Sobradinho, and Itaipú, which characterizes much uncertainty in this variation pattern. The model identifies patterns in the mean and low-frequency bands, indicating phase changes in the mean frequency band of Sobradinho and Água Vermelha in the evaluation period associated with minimum points in the low-frequency band, coincident with very dry years in the region.

In Itaipú, the bands differ in the response of NEB and part of Southeast region; therefore, the model suggests a possible reduction trend in the low-frequency band, identified by the model. However, the model suggests a reduction in the mean frequency band since the fourth projected year, which does not happen.

Figure 7 shows the likelihood ratio between WAR model (represented by the median of the scenarios) and the climatology. Comparing the model with the climatology of the time series of streamflow in the NIS, it demonstrates gain in most of projections over the country between 5 and 10 years. In southern Brazil, the model presents a best performance than climatology in most of BPs in until 4 years of projection; after this projection time, the model loses efficiency, that is, the climatology has a better performance in most of BPs.

It is noteworthy that, in regions strongly influenced by ENSO-driven interannual variability, like the northern and southern Brazil, several BPs exhibit likelihood ratio < 1 in projection periods above 4 years, highlighting the south region. Further of this ENSO-driven interannual variability, Jesus et al. (2016) pointed that the weather and climate in some regions of Brazil, more specifically in the southeastern South America, have a strong relation with Cold Fronts (CFs), which act on a smaller timescale (synoptic scale) from that considered in the WAR model (interannual). These abovementioned two points may have affected the performance of the model in these regions.

Figure 8 shows the projections for the years from 2017 to 2026 of the WAR models for the Água Vermelha, Sobradinho, and Itaipú stations. For Sobradinho, the model indicates above the historical average flow, probably associated with the end of the warm phase of both PDO and AMO. Água Vermelha responds in a similar way, however, with a maximum lag in the mean frequency band from 3 to 4 years regarding to Sobradinho. In contrast, in Itaipú, the model suggests reduction in the low-frequency band, which suggests reduction in the south sector of the country.

Discussion and Conclusions

In this study, time series analyses showed different behaviors in the annual average flow regarding the trend in the period from 1931 to 2016, depending on the region of hydroelectric sector. There is a positive trend in the South region and a negative trend in the Northeast region of the country. Meanwhile, in the North and Midwest regions, most of the exploitations do not present a meaningful trend.

The series of average annual flow also showed traces of interannual and decadal variability. This pattern can be associated with temperature oscillations in the surface of Pacific and Atlantic Oceans. Most of the low- and mean frequency modes are related to the PDO and significantly affect the flow regime in the stations of the NIS. The analysis presented in this study indicates that there are changes in flow values coinciding with changes in the PDO index. Therefore, there is a correlation between the PDO index and the changes in the level of the average annual flow for most of the analyzed stations and more strongly for the stations in the North and Northeast sectors of the NIS. For this reason, the stationarity hypothesis of the streamflow series can be discarded in several NIS locations.

The WAR model can recognize the various patterns of the streamflow time series in the Brazilian electric sector and project

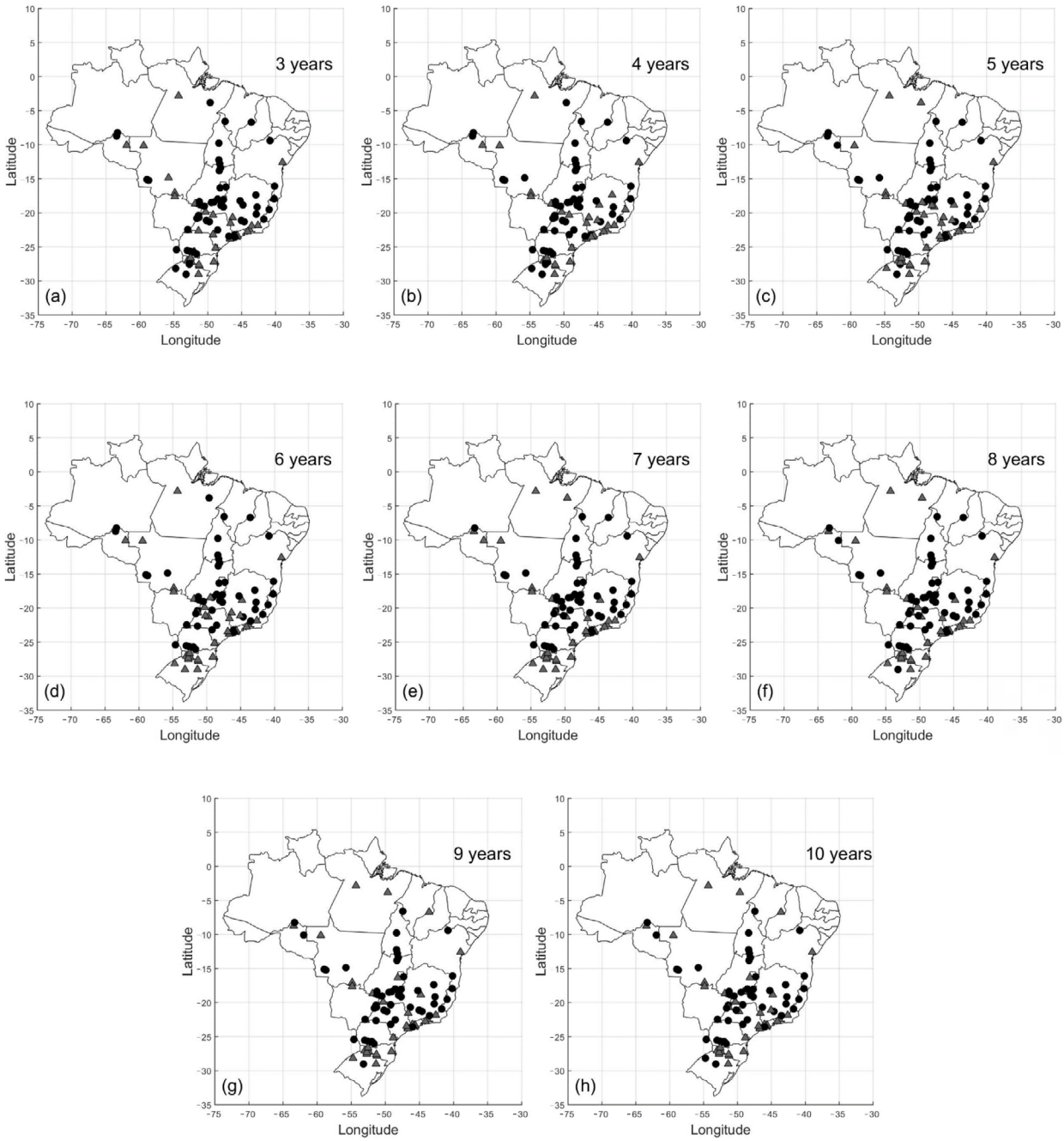

Figure 7 – Likelihood ratios between the WAR model and the climatology for the base posts of NIS. Likelihood ratios > 1 are represented by black circles and < 1 by gray triangles.

the subsequent years. This model presented a better performance than the climatology in most of NIS stations analyzed, indicating that it can be used by managers in the planning of energetic policies and in the search of measures that minimizes the impacts of climate variability on society. In contrast, several BPs in the North and South regions of Brazil presented worse performance than the climatology. It is worth mentioning that these regions are strongly influenced by ENSO-driven interannual climate variability. Furthermore, phenomena that act in a smaller timescale from that considered in the WAR model, such as CFs in synoptic scale, influence the climate in some regions of Brazil. Thus, it is supposed that these points could be responsible for the lower performance of the model in some Brazilian regions, especially the South region of Brazil.

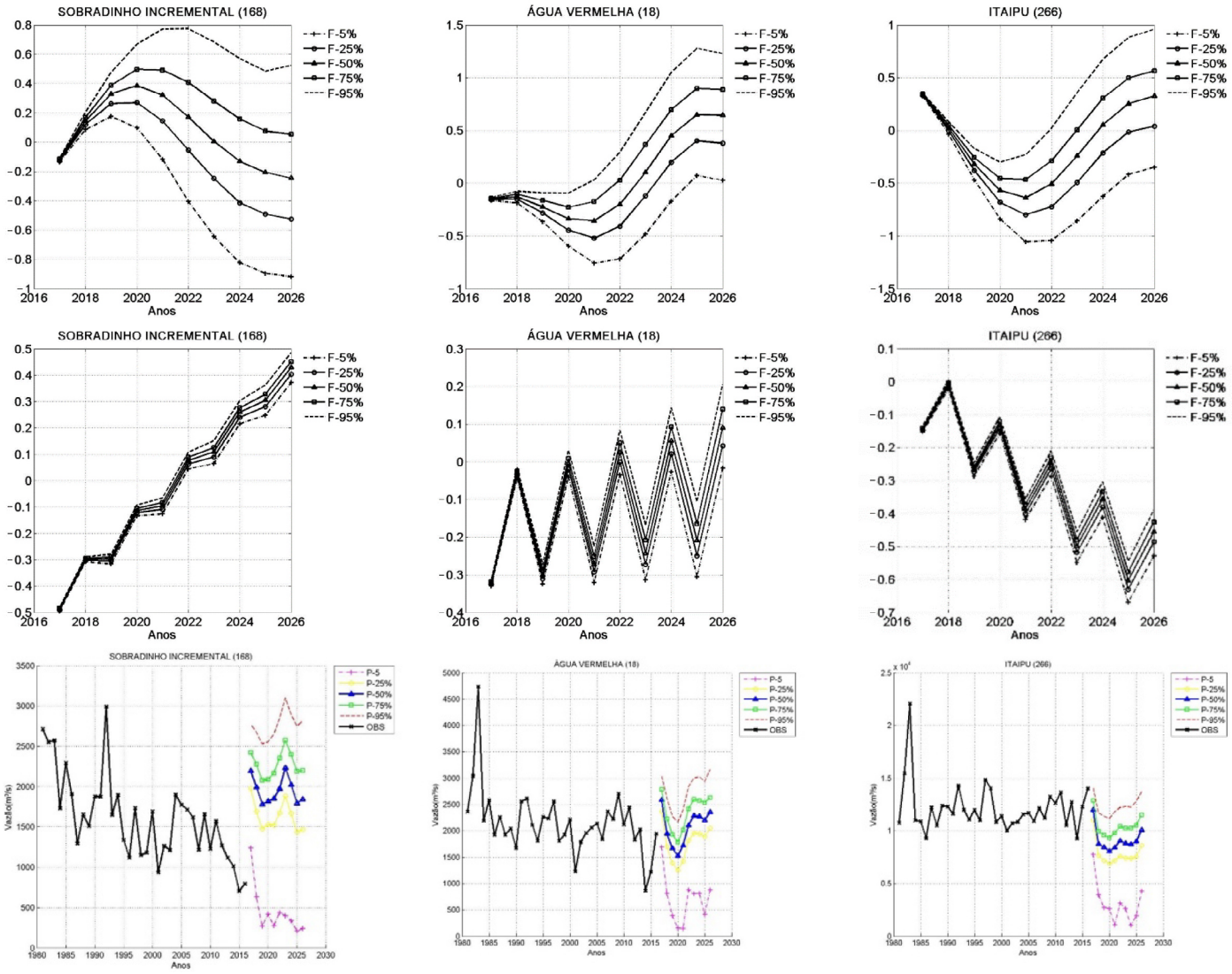

Figure 8 – WAR model streamflow projections for the period from 2017 to 2026.

This methodology permits the evaluation of the flow guarantees and regularization considering the non-stationarity of the time series due to the low-frequency variability, thereby enabling assessment of the guarantees in granting water use and dynamically dealing with the risk.

The energy growth projections indicate that its expansion occurs mainly in Northern Brazil. Therefore, it is necessary to account for the climate variability as one possible element of reduction or increase in the energy supply of the region. Furthermore, it is fundamental that the Brazilian energy growth policy regard, for a long-term energy security, mitigation strategies of both climate change and climate variability impact, an improvement of energetic efficiency, and an increased participation of renewable sources of electricity in the Brazilian energy matrix, which do not have a high sensibility to climate variability.

Contribution of authors:

Lima, C.E.S.: Conceptualization, Methodology, Validation, Software, Formal analysis, Investigation, Resources, Data curation, Writing — original draft, Writing — review and editing. Silva, M.V.M.: Software, Formal analysis, Investigation, Resources, Data curation, Writing — review and editing. Silveira, C.S.: Conceptualization, Methodology, Validation, Software, Formal analysis, Investigation, Resources, Data curation, Writing — original draft, Writing — review and editing, Visualization, Supervision. Vasconcelos Júnior, F.C.: Writing — review and editing, Visualization, Supervision.

References

Alves, B.C.C.; Souza Filho, F.A.; Silveira, C.S., 2013. Análise de tendência e Padrões de Variação das séries históricas de vazões do Operador Nacional de Sistemas (ONS). Revista Brasileira de Recursos Hídricos, v. 18, (4), 19-34. http://dx.doi.org/10.21168/rbrh.v18n4.p19-34.

Costa, F.S.; Maceira, M.E.P.; Damázio, J.M., 2007. Modelos de previsão hidrológica aplicados ao planejamento da operação do sistema elétrico brasileiro. Revista Brasileira de Recursos Hídricos, v. 12, (3), 21-30. http://dx.doi.org/10.21168/rbrh.v12n3.p21-30.

Grimm, A.M.; Almeida, A.S.; Beneti, C.A.A.; Leite, E.A., 2020. The combined effect of climate oscillations in producing extremes: the 2020 drought in southern Brazil. Revista Brasileira de Recursos Hídricos, v. 25, e48. https://doi.org/10.1590/2318-0331.252020200116.

Grimm, A.M.; Saboia, J.P.J., 2015. Interdecadal variability of the south american precipitation in the monsoon season. Journal of Climate, v. 28, (2), 755-775. http://dx.doi.org/10.1175/JCLI-D-14-00046.1.

International Energy Agency – IEA, 2020. World Energy Balances 2020 edition. International Energy Agency (Accessed August 25, 2021) at: https://www.iea.org/countries/brazil.

Jesus, E.M.; Rocha, R.P.; Reboita, M.S.; Llopart, M.; Dutra, L.M.M.; Remedio, A.R.C., 2016. Contribution of cold fronts to seasonal rainfall in simulations over the southern La Plata Basin. Climate Research, v. 68, (2-3), 243-255. http://dx.doi.org/10.3354/cr01358.

Kayano, M.T.; Andreoli, R.V.; Garcia, S.R.; Souza, R.A.F., 2018. How the two nodes of the tropical Atlantic sea surface temperature dipole relate the climate of the surrounding regions during austral autumn. International Journal of Climatology, v. 38, (10), 3927-3941. http://dx.doi.org/10.1002/joc.5545.

Kayano, M.T.; Andreoli, R.V.; Souza, R.A F., 2019. El Niño–Southern oscillation related teleconnections over South America under distinct Atlantic multidecadal oscillation and Pacific interdecadal oscillation backgrounds: La Niña. International Journal of Climatology, v. 39, (3), 1359-1372. http://dx.doi.org/10.1002/joc.5886.

Mantua, N.J.; Hare, S.R.; Zhang, Y.; Wallace, J.M.; Francis, R.C., 1997. A Pacific Interdecadal climate oscillation with impacts on salmon production. Bulletin of American Meteorology Society, v. 78, (6), 1069-1980. https://doi.org/10.1175/1520-0477(1997)078%3C1069:APICOW%3E2.0.CO;2.

Moreira, J.G.V.; Naghettini, M., 2016. Detecção de tendências monotônicas temporais e relação com erros dos tipos I e II: estudo de caso em séries de precipitações diárias máximas anuais do estado do Acre. Revista Brasileira de Meteorologia, v. 31, (4), 394-402. https://doi.org/10.1590/0102-778631231420140155.

Morettin, P.A., 1999. Ondas e ondaletas: da análise de Fourier à análise de ondaletas. Edusp, São Paulo.

Operador Nacional do Sistema – ONS, 2010a. Critérios para estudos hidrológicos – Submódulo 23.5. Procedimentos de Rede. Operador Nacional do Sistema, Brasília, 11 pp.

Operador Nacional do Sistema – ONS, 2010b. Operação do Sistema Interligado Nacional – Relatório Anual de Avaliação das Previsões de Vazões. Operador Nacional do Sistema, Brasília, 230 pp.

Operador Nacional do Sistema – ONS, 2016. O que é o SIN (Sistema Interligado Nacional). Operador Nacional do Sistema, Rio de Janeiro (Accessed Novemer 25, 2021) at: http://www.ons.org.br/paginas/sobre-o-sin/o-que-e-o-sin.

Rocha, R.V.; Souza Filho, F.A., 2020. Mapping abrupt streamflow shift in an abrupt climate shift through multiple change point methodologies: Brazil case study. Hydrological Sciences Journal, v. 65, (16), 2783-2796. https://doi.org/10.1080/02626667.2020.1843657.

Terrier, M.; Perrin, C.; Lavenne, A.; Andréassian, V.; Lerat, J.; Vaze, J., 2021. Streamflow naturalization methods: a review. Hydrological Sciences Journal, v. 66, (1), 12-36. https://doi.org/10.1080/02626667.2020.1839080.

Torrence, C., Compo, G.P., 1998. A practical guide to wavelet analysis. Bulletin of American Meteorology Society, v. 79, 61-78. https://doi.org/10.1175/1520-0477(1998)079%3C0061:APGTWA%3E2.0.CO;2.

Wang, Y.L.; Hsu, Y.C.; Lee, C.P.; Wu, C.R., 2019. Coupling influences of ENSO and PDO on the inter-decadal SST variability of the ACC around the Western South Atlantic. Sustainability, v. 11, (18), 4853. https://doi.org/10.3390/su11184853.

Wang, H.; Kumar, A.; Wang, W.; Xue, Y., 2012. Influence of ENSO on Pacific decadal variability: an analysis based on the NCEP Climate Forecast System. Journal of Climate, v. 25, 6136-6151. https://doi.org/10.1175/JCLI-D-11-00573.1.

Zhang, R.; Delworth, T.L., 2006. Impact of Atlantic multidecadal oscillations on India/Sahel rainfall and Atlantic hurricanes. Geophysical Research Letters, v. 33, (17). https://doi.org/10.1029/2006GL026267.

Zhang, Y.; Wallace, J.M.; Battisti, D., 1997. ENSO-like interdecadal variability: 1900-93. Journal of Climate, v. 10, 1004-1020. https://doi.org/10.1175/1520-0442(1997)010%3C1004:ELIV%3E2.0.CO;2.